Thickness Dependence of the Ambipolar Charge Transport Properties in Organic Field-Effect Transistors based on a Quinoidal Oligothiophene Derivative

ARTICLE *in* THE JOURNAL OF PHYSICAL CHEMISTRY C · OCTOBER 2011

Impact Factor: 4.77 · DOI: 10.1021/jp206129g

6 AUTHORS, INCLUDING:

Jean Charles Ribierre
Kyushu University
60 PUBLICATIONS **562** CITATIONS
SEE PROFILE

Satoshi Watanabe
Kumamoto University
26 PUBLICATIONS **195** CITATIONS
SEE PROFILE

THE JOURNAL OF PHYSICAL CHEMISTRY C

ARTICLE

pubs.acs.org/JPCC

Thickness Dependence of the Ambipolar Charge Transport Properties in Organic Field-Effect Transistors based on a Quinoidal Oligothiophene Derivative

J. C. Ribierre,*[,†,‡] S. Watanabe,[†,§] M. Matsumoto,[§] T. Muto,[†] D. Hashizume,[†] and T. Aoyama*[,†]

[†]RIKEN Advanced Science Institute, 2-1 Hirosawa, Wako, Saitama 351-0198, Japan

[‡]Department of Physics, Ewha Womans University, Seoul 120-750, Korea

[§]Department of Materials Science and Technology, Tokyo University of Science, Yamazaki 2641, Noda 278-8510, Japan

ABSTRACT: We examine the influence of film thickness on the optical and ambipolar field-effect transistor properties of solution-processed dicyanomethylene-substituted quinoidal oligothiophene [QQT(CN)4] thin films. Threshold voltages for both p- and n-channels show a linear thickness dependence due to an increase in the bulk conductance in thicker films. Electron mobility is found to increase gradually when decreasing film thickness. In contrast, hole mobility remains nearly unchanged except in films thinner than 50 nm. Film morphology is characterized by atomic force microscopy and X-ray diffraction techniques. Direct correlation between crystalline grain size and thickness dependence of the electron field-effect mobility is observed. This result can be attributed to a strong effect of the grain boundaries on the electron trapping properties and suggests the possibility to improve the charge transport properties of QQT(CN)4 thin films by controlling their morphology. The influence of contact resistance effects on the electron transport properties of the devices is also discussed. Devices with optimized structure show hole and electron mobilities in the saturation regime as high as 0.08 and 0.015 $cm^2/(V\,s)$, respectively. Overall, this study provides new important insight into the ambipolar charge transport properties of quinoidal oligothiophene derivatives for organic field-effect transistors.

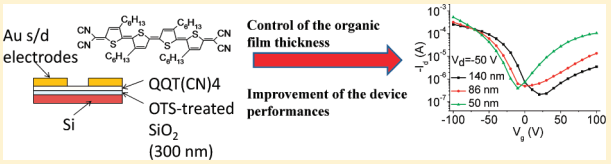

1. INTRODUCTION

Over the past decade, solution-processable organic semiconductors have received considerable attention due to their promising potential for low cost flexible printable optoelectronic devices including light-emitting diodes, solar cells, and organic field-effect transistors (OFETs). In particular, ambipolar organic materials have recently been the subject of intensive research for their application in complementary logic circuits and light-emitting transistors.[1−7] The use of ambipolar transistors, which work as either n-channel or p-channel devices depending on the operating gate voltage, can lead to a significant simplification of device fabrication and integrated circuit design. Ambipolar transport in solution-processed OFETs has been previously demonstrated in interpenetrating blends of p- and n-type materials[2,8−10] as well as in a few single organic semiconductors.[2,3,11−14] However, field-effect mobilities in these materials remain generally low compared with those measured in the best unipolar OFETs and must be improved for the development of practical electronic applications.

Quinoidal oligothiophene derivatives have been studied as n-type and ambipolar organic semiconductors and have shown great promise for the realization of OFETs.[15−21] Recently, we reported high-performance air-stable solution-processed ambipolar OFETs based on a low bandgap dicyanomethylene-substituted quinoidal quaterthiophene derivative [QQT(CN)4] with high hole and electron field-effect mobilities (up to 0.1 and 0.006 $cm^2/(V\,s)$, respectively).[22] This organic semiconducting material exhibits a low bandgap of ∼0.9 eV in the solid state, which enables efficient hole and electron injection from Au drain/source electrodes. Conversion from ambipolar p-type dominant to n-type behavior accompanied by changes in the highest occupied molecular orbital (HOMO) and lowest unoccupied molecular orbital (LUMO) levels were achieved by either a simple thermal annealing or direct laser writing.[22−25] In addition, reversible majority carrier type conversion was reported in QQT(CN)4 by a solvent vapor treatment.[26] These unique phenomena were explained by strong changes in molecular packing and were used to realize solution-processed complementary organic logic circuits based on a monolithic organic semiconductor.[27]

It is now well-established that film solution-processing conditions can play an important role in both morphology of semiconducting organic thin films at the interface with the gate dielectric and the OFET characteristics.[28−33] In this manuscript, we report on the QQT(CN)4 film thickness dependence of ambipolar OFET characteristics and optical properties. The thickness of the QQT(CN)4 semiconducting layer strongly affects the values of the threshold voltage V_{th} and electron field-effect mobilities. Whereas the linear relationship between V_{th} and film thickness is explained by taking into account an increase in bulk conductivity in QQT(CN)4 thicker films, changes in film morphology are responsible for the observed thickness dependence of the

Received: June 29, 2011
Revised: September 6, 2011
Published: September 14, 2011

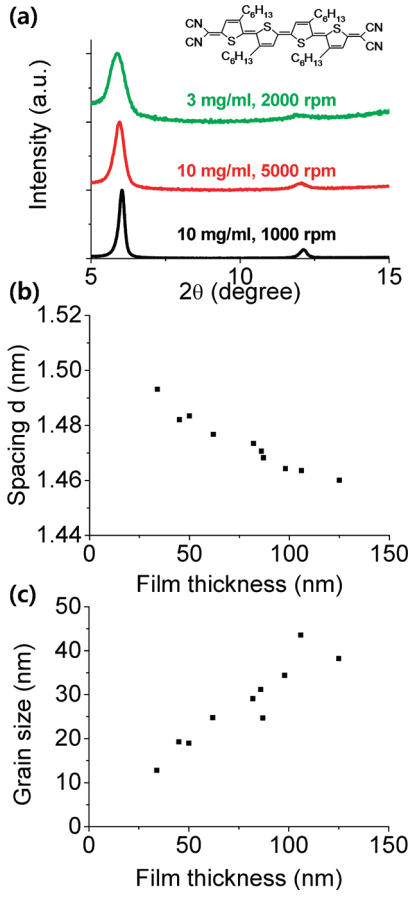

Figure 1. (a) XRD patterns measured in spin-coated QQT(CN)4 neat films with different thicknesses and prepared under different spin-coating conditions. The chemical structure of QQT(CN)4 is shown in the inset. (b) The *d* spacing deduced from the position of the first-order diffraction peak is plotted against film thickness. (c) The diameter of the grain size calculated from the XRD patterns using the Scherrer formula is plotted against film thickness.

electron conduction. The decrease in electron field-effect mobilities with increasing film thickness can be due either to contact resistance effects or to a larger size of the crystal grains in thicker films, resulting in a larger concentration of defects/traps that are located at the grain boundaries. Optimization of the QQT(CN)4 film thickness leads to a notable improvement of the electron field-effect mobility up to 0.015 $cm^2/(V\,s)$ without any changes in hole transport. In addition, the results demonstrate the possibility to tune finely the ambipolar transport properties of QQT(CN)4 thin films without using any thermal or solvent vapor treatment.[23,26] This study provides new useful guidelines for the fabrication of high-performance OFETs and organic integrated circuits based on solution-processable ambipolar materials.

2. EXPERIMENTAL METHODS

The organic semiconductor QQT(CN)4 was synthesized following an improved synthetic method previously reported in the literature.[34] Its chemical structure is shown in the inset of Figure 1. Top-contact bottom gate QQT(CN)4 OFETs of various thicknesses ranging from 26 to 140 nm were fabricated on top of heavily doped n-type silicon wafers with thermally grown 300 nm thick SiO_2 layer. The substrates were cleaned in ultrasonic baths of pure water, 2-propanol, acetone and chloroform prior to a cleaning by UV ozone treatment. The SiO_2 surface was passivated by octadecyltrichlorosilane (OTS) treatment. QQT(CN)4 films were then spin-coated from chloroform solution in ambient conditions. Various solution concentrations (3, 5, and 10 mg/mL) and spin-speeds (from 5000 to 1000 rpm) were used to finely control film thickness. Top-contact 25 nm thick gold drain/source electrodes were thermally sublimed through a shadow mask to fabricate four transistors on a same substrate with a 45 μm channel length (L) and a 4 mm channel width (W). Electrical characterization of the devices was carried out at room temperature using a couple of picoammeter/voltage source units (Keithley, model 6487). The field-effect mobilities μ are extracted from the saturation regime in the output characteristics using the standard method and the following equation, $I_d = ((W/2)L)\mu W_i(V_g - V_{th})^2$, where I_d is the drain current, C_i is the capacitance density of the SiO_2 insulating layer, V_g is the gate voltage, and V_{th} is the threshold voltage determined from the plot of $(|I_d|)^{1/2}$ as a function of V_g. The field-effect mobilities in the linear regime are calculated from the gradient of I_d versus V_g at constant source-drain voltage V_d using the equation $\mu_{linear} = (\partial I_d/\partial V_g)(L/WC_iV_d)$. Note that several devices are characterized for each thickness and the mobilities reported in this study have been averaged.

Absorption spectra were measured in an ambient atmosphere using a UV−vis-NIR scanning absorption spectrophotometer (Shimadzu, UV-3100PC). The QQT(CN)4 films were spin-coated onto fused silica substrates. Film thicknesses were determined with a Dektak profilometer (model IIA, ULVAC) and checked with the measured absorbance values. The morphology of QQT(CN)4 films were characterized by X-ray diffraction (XRD) in a conventional reflection ($\theta-2\theta$) configuration mode. XRD profiles were obtained using the X-ray diffractometer (MacScinece MXP21TA-PO) and Cu Kα monochromatic radiation at 1.54184 Å. Tapping mode atomic force microscope (AFM) images were recorded on a Veeco Dimension 3100 scanning probe microscope with a Nanoscope V controller and equipped with a Si coated cantilever (Veeco, model NCH-W, resonance frequency: 261.9 kHz, spring constant: 29−48 N/m).

3. RESULTS

A. Morphology of QQT(CN)4 Thin Films. Morphology of solution-processed organic thin films can greatly depend on the solvents used for the film deposition as well as the solution concentration and spin-coating conditions. It is well-established that the degree of aggregation in solution is often preserved in the solid state.[35] Information on film morphology and polycrystallinity in QQT(CN)4 neat films was obtained by XRD measurements. Figure 1a shows the normalized XRD profiles measured in several thin films with different thicknesses. The observation of the first-and second-order diffraction peaks indicates that QQT(CN)4 thin films present a good crystallinility and are highly oriented. As displayed in Figure 1b, the position of the primary peak depends on film thickness. The interlayer spacing *d* was calculated from the XRD profiles to decrease gradually from 1.49 to 1.46 nm when increasing film thickness from 34 to 125 nm. It is interesting to note that this *d* value approaches the length of the *c* axis measured by XRD in QQT(CN)4 powder. These results suggest that a better crystallinity is obtained when increasing film thickness. In other words, when the film is thick enough, the effect of the substrate on the molecular packing is

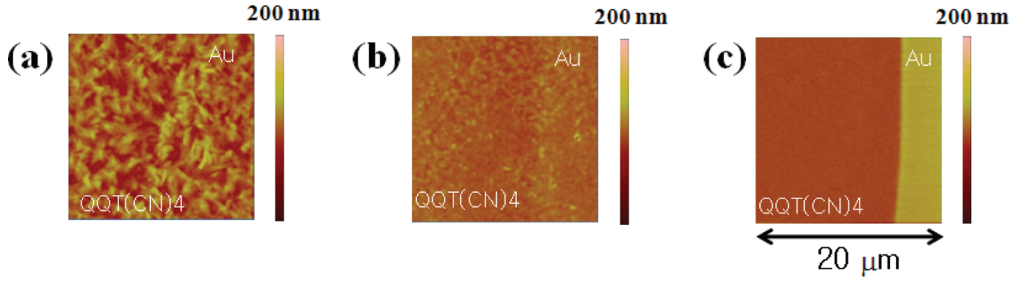

Figure 2. AFM surface topograph,y images of several QQT(CN)4 neat films. Film thicknesses were (a) 86 (10 mg/mL, 3000 rpm), (b) 62 (5 mg/mL, 3000 rpm), and (c) 26 nm (3 mg/mL, 5000 rpm).

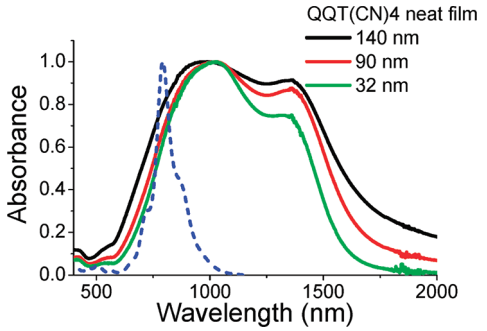

Figure 3. Normalized absorption spectra of QQT(CN)4 in chloroform solution (blue dashed line) and in neat films. The film thicknesses are 140 (spin-coated from a 10 mg/mL solution at 1000 rpm), 90 (5 mg/mL, 1000 rpm), and 32 nm (2 mg/mL, 1000 rpm).

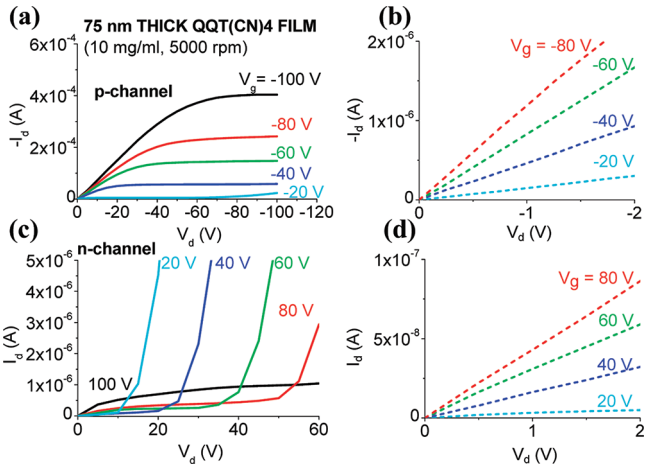

Figure 4. (a,b) p-Channel and (c,d) n-channel output characteristics at various gate voltages measured in air in an OFET based on a 75 nm thick QQT(CN)4 thin film spin-coated at 5000 rpm from a 10 mg/mL chloroform solution. Channel length was 45 μm and the width was 4000 μm.

minimized and the film shows the crystalline properties of the bulk material. To obtain more information on the grain formation in QQT(CN)4 thin films, we extracted the average crystallite size of the grains as a function of film thickness using the full width half-maximum analysis of the primary diffraction peaks and the Scherrer formula.[36] The results are shown in Figure 1c and clearly indicate that the average size of the grains increases monotically and continuously with the film thickness. The values of the diameter of the crystallites were found to be ~12 and 40 nm in 34 and 125 nm thick films, respectively. Figure 2 shows the 20 × 20 μm^2 tapping mode AFM topographic images of several QQT(CN)4 neat films prepared from various solution-processing conditions. The images indicate that the samples have different surface morphology. The surface of the 86 nm thick film spin-coated from a 10 mg/mL solution at 3000 rpm presents the largest crystalline grains. Both grain size and density notably decrease in the 62 nm thick film deposited from a 5 mg/mL solution at 3000 rpm. Finally, the thinnest film (3 mg/mL, 5000 rpm) with a thickness of 26 nm shows a smooth surface without any observable polycrystalline structures. Such a dependence of the surface morphology is in good agreement with the data obtained from the XRD profiles. Overall, the results demonstrate changes in film morphology with a continuous variation of the size of the crystalline grains as a function of film thickness.

B. Absorption Spectra of QQT(CN)4 in Solution and Thin Films. The absorption spectrum of QQT(CN)4 in chloroform solution, shown in Figure 3, presents an intense absorption band in the near-infrared region with a well-defined vibronic structure and a peak maximum at 790 nm. The low bandgap of QQT(CN)4 has been previously assigned to the quinoidal conjugation structure of the oligothiophene backbone.[16,37,38] The absorption spectra measured in the solid state are much broader and exhibit a peak maximum at around 1000−1030 nm. The films do not absorb light significantly in the visible, which can be of interest for the future development of fully transparent electronic devices. The differences observed between the absorption spectra in solution and thin films are related to the polycrystallinity of the films.[22,23] It can also be seen that the absorption spectra become narrower in thinner films. The maximum peak is slightly shifted toward the long wavelengths, whereas the intensity of the shoulder decreases when decreasing film thicknesses. This behavior is presumably due to the thickness dependence of the crystal grain formation. Because a better crystallinity is observed in thicker films, it is reasonable to assume that aggregation and intermolecular interactions in the grains become stronger as the film thickness is increased, resulting in the observed changes in the absorption spectra.

C. Characterization of QQT(CN)4 Organic Transistors. Figure 4 shows the p-channel and n-channel output characteristics of a 75 nm thick QQT(CN)4 OFET with top-contact Au source/drain electrodes. The device exhibits good ambipolar transport with both hole and electron enhancement modes. For negative V_g, only holes are injected and accumulated in the QQT(CN)4 layer. In this voltage range, the drain current I_d reaches saturation at high V_d, and the device operates as a p-channel transistor. For positive V_g and high V_d values, both electrons and holes are accumulated in the channel. In that case, the drain current I_d does not reach saturation and rapidly increases with V_d. This

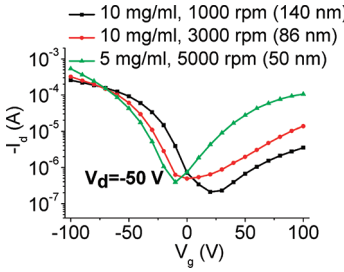

Figure 5. Transfer characteristics of QQT(CN)4 OFETs with organic thin film thicknesses of 140 (10 mg/mL, 1000 rpm), 86 (10 mg/mL, 3000 rpm), and 50 nm (5 mg/mL, 5000 rpm). These measurements were carried out in air with $V_d = -50$ V. Channel length was 45 μm, and the width was 4000 μm.

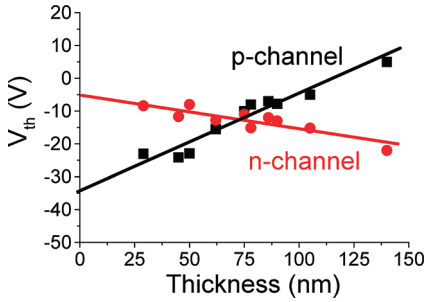

Figure 6. Thickness dependence of threshold voltage V_{th} measured in the p- (black) and n- (red) channels of QQT(CN)4 OFETs.

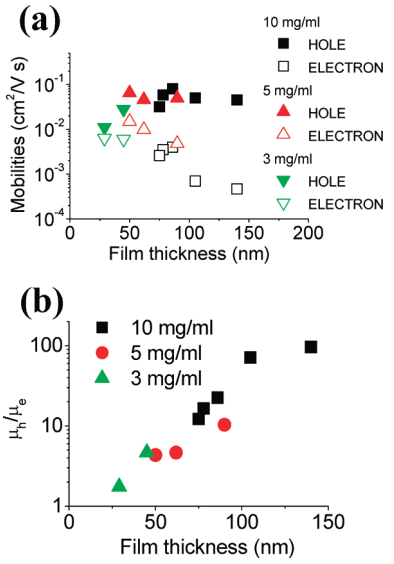

Figure 7. (a) Thickness dependence of the hole (solid) and electron (open) field-effect mobilities in QQT(CN)4 OFETs. The QQT(CN)4 thin films were spin-coated from 10 (black), 5 (red), and 3 mg/mL (green) chloroform solution at spin-speeds varying from 1000 to 5000 rpm. (b) Thickness dependence of the ratio between hole (μ_h) and electron (μ_e) mobilities.

superlinear dependence of I_d with V_d is expected for ambipolar transistors and is found to be very pronounced in the n-channel of our devices. Overall, the shape of the measured output characteristics is a direct consequence of the fact that the QQT(CN)4 OFETs are p-type dominant ambipolar devices with high hole field-effect mobilities. It is also worth noting that the output characteristics measured at low negative and positive V_d in all samples show the expected linear behavior.[39]

Figure 5 shows the influence of the film thickness on the transfer characteristics of QQT(CN)4 OFETs operating in air at $V_d = -50$ V. All of these transistors exhibit clear ambipolar transport with the typical V-shaped characteristics, one arm being related to hole transport and the other one to electron transport. The hole current measured at negative V_g presents similar features indicating that hole conduction in these devices does not depend significantly on film thickness. In contrast, the drain current at positive V_g, which is associated with electron transport notably changes with thickness by almost two orders of magnitude, implying a strong thickness dependence of the electron field-effect mobility, the threshold voltage, or both. The consequence of this behavior is a decrease in the on/off current ratio for the electron current with increasing film thickness, in contrast with what is observed for the hole current. It can also be seen directly from the transfer characteristics that indeed the threshold voltages associated with n- and p-channels vary with the thickness of the QQT(CN)4 thin film.

Figure 6 shows the evolution of the threshold voltages V_{th} calculated from the transfer characteristics as a function of the QQT(CN)4 film thickness. For the p-channel, V_{th} was found to increase linearly with film thickness from −24 to 5 V. In the case of the n-channel, a linear decrease in V_{th} from −9 to −22 V was observed when increasing film thickness from 29 to 140 nm. Such a linear thickness dependence of V_{th} has been previously reported in the p-channel of both pentacene[40] and polythiophene[41] OFETs and is related to an increase in the bulk conductance with film thickness. Threshold voltage is a critical parameter in the operation of OFETs, and its thickness dependence has been previously described by the equation:[41] $V_{th} = qp_0d/C_i + V_0$, where q is the charge of the electron or hole, p_0 corresponds to the bulk charge density, V_0 is related to the flat band potential of the semiconductor, C_i is the capacitance of the insulating layer, and d denotes the thickness of the organic semiconductor layer. The linear fits of the experimental data shown in Figure 6 lead to bulk-charge density values for holes and electrons equal to 2.5×10^{17} and 7.8×10^{16} cm^{-3}, respectively. This result seems to be in good agreement with the fact that QQT(CN)4 thin films exhibit an ambipolar p-type dominant behavior. Overall, these results suggest that the threshold voltage in top-contact ambipolar OFETs can be finely tuned by simply controlling the thickness of the semiconducting active layer.

Figure 7a shows the hole and electron field-effect mobilities determined from the transfer characteristics in the saturation regime as a function of the QQT(CN)4 film thickness. For thicknesses varying from 50 to 140 nm, hole mobilities do not show any clear thickness dependence with measured values in the range of 0.07 ± 0.03 $cm^2/(V\ s)$. In contrast, electron mobilities are found to increase gradually with decreasing film thickness from 5×10^{-4} to 0.015 $cm^2/(V\ s)$. In thinner films, both hole and electron mobilities are lower, reaching 0.01 and 0.006 $cm^2/(V\ s)$, respectively, in the 29 nm thick film. This could be simply due to an increase in defect density or higher leak current when reducing film thickness. We also found that the ratio between hole and electron mobilities measured in our devices monotonically increases with film thickness from 1.7 to nearly 100 (Figure 7b). The linear and saturation field-effect mobilities for both holes and electrons are then compared for four different thicknesses of QQT(CN)4 films, and these values are listed in the Table 1. It can be seen that

dx.doi.org/10.1021/jp206129g |J. Phys. Chem. C 2011, 115, 20703–20709

Table 1. Comparison of the Hole and Electron Field-Effect Mobilities Measured in the Saturation and Linear Regimes As Function of the QQT(CN)4 Film Thickness

d (nm)	$\mu_{h,lin}$ ($cm^2/(V\,s)$)	$\mu_{h,sat}$ ($cm^2/(V\,s)$)	$\mu_{e,lin}$ ($cm^2/(V\,s)$)	$\mu_{e,sat}$ ($cm^2/(V\,s)$)
140	0.04	0.045	9.5×10^{-5}	4.5×10^{-4}
86	0.05	0.08	5×10^{-4}	0.004
75	0.04	0.03	8.5×10^{-4}	0.003
50	0.06	0.065	0.006	0.015

the hole mobility remains nearly the same in both regimes and thus does not change substantially with film thickness. In contrast, we find that the electron mobility in the linear regime is lower than that in the saturation regime, but their thickness dependence follows exactly the same trend. Although the mobility values measured in the linear regime are known to be more accurate,[42] such differences between the linear and saturation mobility values are generally assigned to contact resistance effects.[39,43] This finding suggests that the electron transport in QQT(CN)4 OFETs is more affected by contact resistance effects than the hole conduction properties. These results provide clear evidence that the characteristics of ambipolar QQT(CN)4 OFETs can be controlled by adjusting the film thickness of the active semiconducting layer. Devices based on a 50 nm thick QQT(CN)4 neat film show optimum performance with balanced hole and electron mobilities of and 0.015 $cm^2/(V\,s)$ respectively in the saturation regime. Note that the best electron field-effect mobility found in the present study is substantially higher than the value previously reported of 0.006 $cm^2/(V\,s)$ in OFETs based on a 90 nm QQT(CN)4 thin film.[22] Overall, these results confirm that solution-processable quinoidal oligothiophene derivatives are very attractive candidates for organic electronic applications.

4. DISCUSSION

Thickness dependence of the charge carrier mobilities in unipolar top-contact OFETs has been reported in a large variety of devices based on different organic semiconducting materials including pentacene,[40,44−46] rubrene,[47] phthalocyanine,[48] polythiophene,[49] and perylene derivatives.[50] In particular, optimum film thicknesses of 30[46] and 120 nm[47] were observed in top-contact pentacene- and rubrene-based OFETs, respectively. In the case of top-contact OFETs, charge injection from source and drain electrodes to the conduction channel depends on both the interface charge injection from the metal contact to the organic semiconductor and the vertical charge transport through the organic thin film to the channel. The total contact resistance of the devices thus corresponds to the sum of the interface contact resistance and the vertical bulk resistance for both source and drain electrodes. The decrease in field-effect mobilities in thick films was often assigned to an increase in the vertical bulk resistance with thickness. In the case of pentacene, the proposed explanation was based on the vertical transport, which takes place perpendicularly to the π-overlapped direction of the molecular layer structure. More recently, an increasing contact resistance and decreasing charge carrier mobilities for both p-type and n-type OFETs were observed when increasing the thickness of the organic semiconducting thin film.[50] However, this work demonstrated that the thickness dependence of the field-effect mobilities in OFETs could not be assigned to contact resistances and was essentially due to morphological effects in the channel of the organic semiconducting thin films. In the case of ambipolar QQT(CN)4 OFETs, the results suggest some contact resistance effects[51−53] on the electron transport properties. Because the injection barrier is certainly higher for electrons than for holes, we cannot exclude the possibility that these contact resistance effects could be the reason for the observed thickness dependence of the electron mobilities. The decreased electron field-effect mobilities in QQT(CN)4 thicker films could indeed be due to the charge injection efficiency and a highly resistive vertical transport of electrons and the longer distance between the Au electrode and the QQT(CN)4/SiO_2 interface resulting in an increase in the contact resistance. In parallel, the thickness independence of the hole field-effect mobilities in QQT(CN)4 films thicker than 50 nm supports a high vertical hole mobility and hence a negligible bulk resistance in the vertical direction.

Solution-processing conditions can potentially have an influence on the alignment of the QQT(CN)4 molecules at the interface with the dielectric layer. A better orientation[54,55] of the molecules in thinner films could lead to a significant increase in the electron mobility with decreasing film thickness but would also affect hole transport. Previous work has also suggested that ambipolar OFET properties of dicyanomethylene-substituted oligothiophenes strongly depend on the quinoidal or aromatic character of their conjugation paths.[17] The absence of changes in the Raman spectra (data not shown) provides clear evidence that the thickness dependence of field-effect mobilities is not due here to any unexpected modifications in the conjugation structure with film thickness and solution-processing conditions. However, the thickness dependence of the charge transport properties in QQT(CN)4 OFETs can also be due to the influence of the film morphology on the electron trap density.

Charge transport properties and OFET characteristics are generally improved when the molecular arrangement favors strong intermolecular interactions and $\pi-\pi$ overlap between adjacent molecules. However, in polycrystalline films, grain boundaries that insulate the crystalline domains from the remainder of the films can play the role of energy barriers to charge transport and lead to a decrease in the field-effect mobilities.[56] Di Carlo et al. reported that a large density of carrier traps is present at grain boundaries in top-contact p-type pentacene OFET.[57] Similar observations were made in n-type devices based on thermally evaporated C_{60} and perylene derivatives.[58−60] These studies show that larger crystalline grains lead to a reduced number of grain boundaries and charge traps, resulting in higher charge carrier mobilities in organic semiconducting thin films. In contrast, we found in QQT(CN)4 films a gradual decrease in the electron mobility when increasing the grain size. However, the sizes of the crystalline grains in spin-coated QQT(CN)4 films are at least one order of magnitude smaller than those measured in these previous studies, which were based on thermally evaporated organic thin films. It is also important to note that other factors such as the depth and the shape of the grain boundaries can play a significant role in the electron trapping processes. The results shown in Figure 1 suggested a better crystallinity of the QQT(CN)4 films when the thickness is increased, and we can reasonably assume that the grain boundaries are narrower and better defined in thicker films. Such grain boundaries can contain more morphological defects related to the creation of electron traps and thus could have a much stronger impact on the electron transport properties, resulting in the observed continuous decrease in electron mobilities when increasing film thickness. Note that

electron trapping in organic thin films is sometimes due to O_2/H_2O molecules that diffuse in the layers through large and deep grain boundaries.[58,60] All device fabrication and characterization in this study were carried out in ambient atmosphere. As previously mentioned, QQT(CN)4 OFETs are highly stable in air, and no striking differences in their electrical performance have been observed when the measurements were performed either in air or under vacuum. From these considerations, the thickness dependence of the electron field-effect mobilities observed in our device cannot be assigned to any oxidative doping, which would become a more severe barrier for electron transport with increasing film thickness. Overall, this work demonstrates the possibility to control precisely the ambipolar transport properties of QQT(CN)4 OFETS not only by a combination of thermal and solvent vapor treatments but also by simply tuning the organic semiconducting film thickness. This study also provides an observation of an optimum film thickness for improving the charge carrier mobilities in ambipolar OFETs, and the results should be taken into account in the further development of high-performance ambipolar organic electronic devices.

5. CONCLUSIONS

We have fabricated solution-processed ambipolar top-contact QQT(CN)4-based OFETs with different organic film thicknesses ranging from 26 to 140 nm to investigate the thickness dependence of the device characteristics. The linear relationship between threshold voltage and film thickness was described by a model based on an increase in the bulk conductance in thicker films. In films thicker than 50 nm, electron field-effect mobilities strongly decrease with film thickness, whereas hole transport properties are not significantly modified. This thickness dependence can be due to either the influence of the grain boundaries on the electron trapping properties or contact resistance effects. The best devices obtained with a 50 nm thick QQT(CN)4 film exhibit hole and electron mobilities of about 0.07 and 0.015 $cm^2/(V\,s)$, respectively. These results confirm that QQT(CN)4 and quinoidal oligothiophene derivatives are attractive ambipolar materials for organic electronic applications. The finding of an optimum film thickness provide new insight into the ambipolar charge transport properties of OFETs. We conclude that these results should be pointed out as an important observation for the optimization and the future development of high mobility ambipolar OFETs.

AUTHOR INFORMATION

Corresponding Author

*Tel: +82-2-3277-4646, Fax: +82-2-3277-2372, E-mail: jcribierre@ewha.ac.kr (J.C.R.). Tel: +81-48-467-4571, Fax: +81-48-467-4571, E-mail: taoyama@riken.jp (T.A.).

ACKNOWLEDGMENT

The research leading to these results has received funding from the Japanese Society for the Promotion of Science via a JSPS KAKENHI grant (no. 22350084).

REFERENCES

(1) Zaumseil, J.; Sirringhaus, H. *Chem. Rev.* **2007**, *107*, 1296.
(2) Meijer, E. J.; de Leeuw, D. M.; Setayesh, S.; Van Veenendaal, E.; Huisman, B.-H.; Blom, P. W. M.; Hummelen, J. C.; Scherf, U.; Klapwijk, T. M. *Nat. Mater.* **2003**, *2*, 678.
(3) Anthopoulos, T. D.; Setayesh, S.; Smits, E.; Cölle, M.; Cantatore, E.; de Boer, B.; Blom, P. W. M.; de Leeuw, D. M. *Adv. Mater.* **2006**, *18*, 1900.
(4) Cornil, J.; Brédas, J. L.; Zaumseil, J.; Sirringhaus, H. *Adv. Mater.* **2007**, *19*, 1791.
(5) Muccini, M. *Nat. Mater.* **2006**, *5*, 605.
(6) Dinelli, F.; Capelli, R.; Loi, M. A.; Murgia, M.; Muccini, M.; Facchetti, A.; Marks, T. J. *Adv. Mater.* **2006**, *18*, 1416.
(7) Kim, F. S.; Guo, X.; Watson, M. D.; Jenekhe, S. A. *Adv. Mater.* **2010**, *22*, 478.
(8) Babel, A.; Wind, J. D.; Jenekhe, S. A. *Adv. Funct. Mater.* **2004**, *14*, 891.
(9) Shkunov, M.; Simms, R.; Heeney, M.; Tierney, S.; McCulloch, I. *Adv. Mater.* **2005**, *17*, 2608.
(10) Tada, K.; Harada, H.; Yoshino, K. *Jpn. J. Appl. Phys., Part 2* **1996**, *35*, L944.
(11) Anthopoulos, T. D.; de Leeuw, D. M.; Cantatore, E.; Setayesh, S.; Meijer, E. J.; Tanase, C.; Hummelen, J. C.; Blom, P. W. M. *Appl. Phys. Lett.* **2004**, *85*, 4205.
(12) Chikamatsu, M.; Mikami, T.; Chisaka, J.; Yoshida, Y.; Shimizu, A.; Kubo, T.; Morita, Y.; Nakasuji, K. *Appl. Phys. Lett.* **2007**, *91*, 043506.
(13) Anthopoulos, T. D.; Tanase, C.; Setayesh, S.; Meijer, E. J.; Hummelen, J. C.; Blom, P. W. M.; de Leeuw, D. M. *Adv. Mater.* **2004**, *16*, 2174.
(14) Cicoira, F.; Coppedé, N.; Iannota, S.; Martel, R. *Appl. Phys. Lett.* **2011**, *98*, 183303.
(15) Pappenfus, T. M.; Chesterfield, R. J.; Frisbie, C. D.; Mann, K. R.; Casado, J.; Raff, J. D.; Miller, L. L. *J. Am. Chem. Soc.* **2002**, *124*, 4184.
(16) Chesterfield, R. J.; Newman, C. R.; Pappenfus, T. M.; Ewbank, P. C.; Haukaas, M. H.; Mann, K. R.; Miller, L. L.; Frisbie, C. D. *Adv. Mater.* **2003**, *15*, 1278.
(17) Ortiz, R. P.; Facchetti, A.; Marks, T. J.; Casado, J.; Zgierski, M. Z.; Kozaki, M.; Hernandez, V.; Lopez Navarrete, J. T. *Adv. Funct. Mater.* **2009**, *19*, 386.
(18) Handa, S.; Miyazaki, E.; Takimiya, K.; Kunugi, Y. *J. Am. Chem. Soc.* **2007**, *129*, 11684.
(19) Suzuki, Y.; Miyazaki, E.; Takimiya, K. *J. Am. Chem. Soc.* **2010**, *132*, 10453.
(20) Handa, S.; Miyazaki, E.; Takimiya, K. *Chem. Commun.* **2009**, 3919.
(21) Suzuki, Y.; Shimawaki, M.; Miyazaki, E.; Osaka, I.; Takimiya, K. *Chem. Mater.* **2011**, *23*, 795.
(22) Ribierre, J. C.; Watanabe, S.; Matsumoto, M.; Muto, T.; Aoyama, T. *Appl. Phys. Lett.* **2010**, *96*, 083303.
(23) Ribierre, J. C.; Fujihara, T.; Watanabe, S.; Matsumoto, M.; Muto, T.; Nakao, A.; Aoyama, T. *Adv. Mater.* **2010**, *22*, 1722.
(24) Ribierre, J. C.; Fujihara, T.; Muto, T; Aoyama, T. *Appl. Phys. Lett.* **2010**, *96*, 233302.
(25) Ribierre, J. C.; Takaishi, K.; Muto, T; Aoyama, T. *Opt. Mater.* **2011**, *33*, 1415.
(26) Ribierre, J. C.; Watanabe, S.; Matsumoto, M.; Muto, T; Nakao, A.; Aoyama, T. *Adv. Mater.* **2010**, *22*, 4044.
(27) Ribierre, J. C.; Fujihara, T.; Muto, T; Aoyama, T. *Org. Electron.* **2010**, *11*, 1469.
(28) Tsao, H. N.; Cho, D.; Wenzel Andreasen, J.; Rouhanipour, A.; Breiby, D. W.; Pisula, W.; Müllen, K. *Adv. Mater.* **2009**, *21*, 209.
(29) Chang, P. C.; Lee, J.; Huang, D.; Subramanian, V.; Murphy, A. R.; Fréchet, J. M. J. *Chem. Mater.* **2004**, *16*, 4783.
(30) Yang, S. Y.; Shin, K.; Park, C. E. *Adv. Funct. Mater.* **2005**, *15*, 1806.
(31) Singh, T. B.; Günes, S.; Marjanovic, N.; Sariciftci, N. S.; Menon, R. *J. Appl. Phys.* **2005**, *97*, 114508.
(32) Kim, C.; Facchetti, A.; Marks, T. J. *Science* **2007**, *318*, 76.
(33) Ribierre, J. C.; Ghosh, S.; Takaishi, K.; Muto, T; Aoyama, T. *J. Phys. D: Appl. Phys.* **2011**, *44*, 205102.
(34) Higuchi, H.; Nakayama, T.; Koyama, H.; Ojima, J.; Wada, T.; Sasabe, H. *Bull. Chem. Soc. Jpn.* **1995**, *68*, 2363.
(35) Nguyen, T. Q.; Doan, V.; Schwartz, B. J. *J. Chem. Phys.* **1999**, *110*, 4068.

(36) Patterson, A. L. *Phys. Rev.* **1939**, *56*, 978.
(37) Casado, J.; Miller, L. L.; Mann, K. R.; Pappenfus, T. M.; Higuchi, H.; Orti, E.; Milian, B.; Pou-Amerigo, R.; Hernandez, V.; Lopez Navarrete., J. T. *J. Am. Chem. Soc.* **2002**, *124*, 12380.
(38) Ribierre, J. C.; Aoyama, T.; Watanabe, S.; Gu, J.; Muto, T.; Matsumoto, M.; Nakao, A.; Wada, T. *Jpn. J. Appl. Phys.* **2010**, *49*, 01AB06.
(39) Cicoira, F.; Aguirre, C. M.; Martel, R. *ACS Nano* **2011**, *5*, 283.
(40) Schroeder, R.; Majewski, L. A.; Grell, M. *Appl. Phys. Lett.* **2003**, *83*, 3201.
(41) Singh, V.; Yano, M.; Takashima, W.; Kaneto, K. *Jpn. J. Appl. Phys.* **2006**, *45*, 534.
(42) Horowitz, G. *J. Mater. Chem.* **1999**, *9*, 2021.
(43) Bain, S.; Smith, D. C.; Wilson, N. R.; Carrasco-Orozco, M. *Appl. Phys. Lett.* **2009**, *95*, 143304.
(44) Gowrisanker, S.; Ai, Y.; Qevedo-Lopez, A.; Jia, H.; Alshareef, H. N.; Vogel, E.; Gnade, B. *Appl. Phys. Lett.* **2008**, *92*, 153305.
(45) Pesavento, P. V.; Puntambekar, K. P.; Frisbie, C. D.; McKeen, J. C.; Ruden, P. P. *J. Appl. Phys.* **2006**, *99*, 094504.
(46) Lee, J.; Kim, K.; Kim, J. H.; Im, S.; Jung, D. Y. *Appl. Phys. Lett.* **2003**, *82*, 4169.
(47) Choi, J. M.; Im, S. *Appl. Phys. Lett.* **2008**, *93*, 043309.
(48) Hoshino, S.; Kamata, T.; Yase, K. *J. Appl. Phys.* **2002**, *92*, 6028.
(49) Jia, H.; Gowrisanker, S.; Pant, G. K.; Wallace, R. M.; Gnade, B. E. *J. Vac. Sci. Technol., A* **2006**, *24*, 1228.
(50) Boudinet, D.; Benwadih, M.; Altazin, S.; Gwoziecki, R.; Verilhac, J. M.; Coppard, R.; Le Blevennec, G.; Chartier, I.; Horowitz, G. *Org. Electron.* **2010**, *11*, 291.
(51) Blanchet, G. B.; Fincher, C. R.; Lefenfeld, M.; Rogers, J. A. *Appl. Phys. Lett.* **2004**, *84*, 296.
(52) Yagi, I.; Tsukagoshi, K.; Aoyagi, Y. *Appl. Phys. Lett.* **2004**, *84*, 813.
(53) Gundlach, D. J.; Zhou, L.; Nichols, J. A.; Jackson, T. N.; Necliudov, P. V.; Shur, M. S. *J. Appl. Phys.* **2006**, *100*, 024509.
(54) Kline, R. J.; McGehee, M. D.; Toney, M. F. *Nat. Mater.* **2006**, *5*, 222.
(55) Umeda, T.; Tokito, S.; Kumaki, D. *J. Appl. Phys.* **2007**, *101*, 054517.
(56) Verlaak, S.; Arkhipov, W.; Heremans, P. *Appl. Phys. Lett.* **2003**, *82*, 745.
(57) Di Carlo, A.; Piacenza, F.; Bolognesi, A.; Stadlober, B.; Maresh, H. *Appl. Phys. Lett.* **2005**, *86*, 263501.
(58) Matsushima, T.; Yahiro, M.; Adachi, C. *Appl. Phys. Lett.* **2007**, *91*, 103505.
(59) Ling, M. M.; Erk, P.; Koenemann, M.; Locklin, J.; Bao, Z. *Adv. Mater.* **2007**, *19*, 1123.
(60) Wen, Y.; Liu, Y.; Di, C.; Wang, Y.; Sun, X.; Guo, Y.; Zheng, J.; Wu, W.; Ye, S.; Yu, G. *Adv. Mater.* **2009**, *21*, 1631.